Auger Electron Ejection from Germanium and Silicon by Noble Gas Ions

HOMER D. HAGSTRUM
Bell Telephone Laboratories, Murray Hill, New Jersey
(Received March 21, 1960)

Experimental results concerning electron ejection from annealed, atomically clean surfaces of germanium and silicon by the singly charged ions of the noble gases are reported. The (111) and (100) faces of silicon and the (111) face of germanium have been studied. Total yield and kinetic energy distribution of ejected electrons were measured and ion energies varied in the range 10 to 1000 ev. A new method of operation of the apparatus and of obtaining the kinetic energy distributions from the recorded retarding potential data has been employed. Documentation of the state of the target surfaces is given including photomicrographs and electron micrographs of the silicon surfaces. Since these experimental results are subsequently to be interpreted theoretically, identification of the results with the theoretical ideas only is given here.

I. INTRODUCTION

THE results of a study of electron ejection from germanium and silicon surfaces by noble gas ions of incident kinetic energies in the range 10 to 1000 ev are reported in this paper. For sufficiently large ionization energy it is in this kinetic energy range that ejection from a solid occurs predominantly by means of the two-electron, Auger-type neutralization of the ion at the surface.

The transitions which give rise to the electrons observed outside the solid involve two electrons which originally reside in the valence band at the surface of the semiconductor. When the approaching ion has come close enough to the surface for the electronic wave functions of atom and solid to overlap, one electron from the valence band tunnels into the ground state of the approaching ion, neutralizing it. A second electron picks up the energy released by the first and becomes an excited (Auger) electron which will leave the solid if it has energy above the surface barrier and is properly directed. In this experiment one measures the total yield and kinetic energy distribution of these ejected electrons as a function of the nature of the ion, its incident kinetic energy, and the state of the solid surface. The results reported here relate in the main to the atomically clean surfaces of germanium and silicon in an annealed condition. Work on the effects of gas adsorption and surface damage on the Auger ejection process will be published later.

This is an experimental paper in which apparatus and experimental conditions (Sec. II) and the methods of measurement (Secs. III and IV) are discussed. A new method of recording and reducing the retarding potential data from which the kinetic energy distributions are obtained has been employed in this work. The preparation and observation of the target surfaces have been carefully documented (Secs. II and V). The basic results of total yield, γ_i, and kinetic energy distribution, $N_0(E_k)$, of electrons ejected from atomically clean (111) and (100) faces of Si and the (111) face of Ge are presented (Secs. III and IV). These are the first studies of Auger ejection from clean surfaces of the elemental semiconductors and constitute an extension of work already reported for the refractory metals.[1]

No attempt is made here to interpret the results theoretically. In other publications the theory of the Auger neutralization process will be extended from metals to semiconductors and machine calculations of the kinetic energy distributions reported. It has been possible to extend the theory for these semiconductors further than that for the refractory metals because of the greater knowledge of their band structure. The

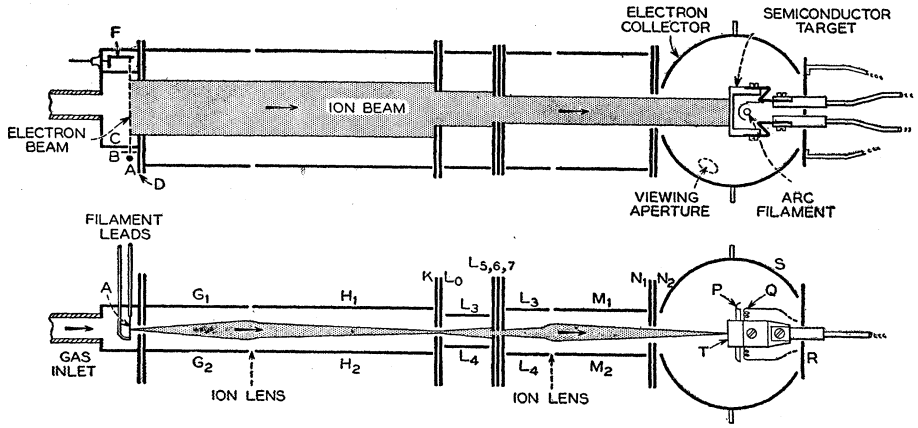

FIG. 1. Schematic diagram of the experimental apparatus. Two views at right angles are shown. For a schematic view of the vacuum envelope see Fig. 1 of reference 3.

[1] H. D. Hagstrum, Phys. Rev. **96**, 325 (1954), **104**, 317 (1956), W; Phys. Rev. **104**, 672 (1956), Mo.

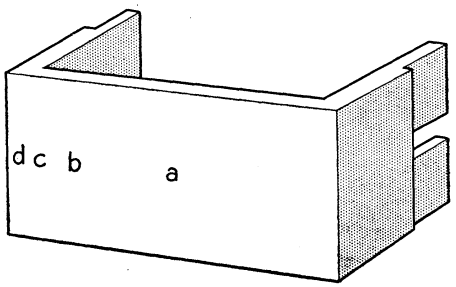

FIG. 2. Shape of target cut from single crystal semiconducting material. The letters on the front face indicate positions at which photographs discussed in Sec. V and shown in Figs. 15–18 were taken. The front face is 14 by 7 mm in size.

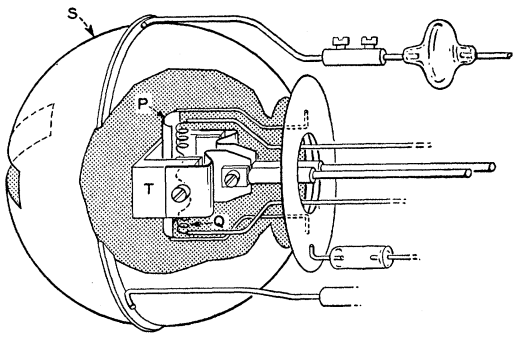

FIG. 3. A cutaway view of the electron collector sphere S, the target T, evaporation shield P, and arc filament Q. The sphere is 4 cm in diameter. The ion beam enters the sphere through the rectangular aperture shown at the left in this figure.

results reported here have been used to determine some features of the valence band structure of the semiconductor and of the interaction of atomic species with its surface. In this paper, however, only a brief identification of the basic results with the theoretical ideas is made (Sec. VI).

II. APPARATUS AND EXPERIMENTAL CONDITIONS

The apparatus used in this work is like others reported earlier.[2] The electrode arrangements are shown schematically in Fig. 1. This instrument is a rebuilt version of that used in the study of the effect of monolayer formation.[3] The glass envelope was modified so that the electron collecting sphere S could be attached to and removed with the target assembly. Also, an arrangement for sputtering the target surface was included.

Briefly, the operation of the apparatus is as follows: Electrons from the filament A traverse the tube in a magnetically collimated beam through apertures in electrodes B and C and are collected at F. Ions formed inside the box C are drawn out through an aperture in D, which is a part of C, and are focused by the lenses G-H and L-M. These lenses are arranged so that cross voltages, as between electrodes H_1 and H_2 or M_1 and M_2, may be applied to adjust the motion of the beam through the apparatus. Appropriate stops are provided to limit the angular spread of the ion beam. The focused ion beam then passes through apertures in N and S without touching these electrodes and falls on the front surface of the target T. Electrons ejected from T are collected at S. S is a sphere of 4-cm diameter.

The semiconductor targets were cut from single crystal material in the geometrical form shown in Fig. 2. These are mounted in the apparatus as is shown in Fig. 1 and in Fig. 3, a close-up of the target chamber. After etching, the front face of the target is 14 mm long, 7 mm wide, and 0.5 mm thick. The legs between the front face and the clamped portion are 4 mm long and 1 mm thick. Three such targets were used in this work. They have been designated Si(100), Si(111), and Ge(111) to indicate the material from which they were cut and the crystallographic direction which is perpendicular, within a few degrees, to the front face of the target. Si(100), Si(111), and Ge(111) were all cut from p-type material of initial resistivity 13.5, 15.0, and 3.3 ohm cm, respectively. Since the resistivity changed as the result of heating during the experiments (Sec. V), the initial characteristics of the target material are of little importance. Furthermore, one does not expect the conductivity type and doping of the sample, or, in fact, the presence of a surface p skin[4] to have any appreciable effect on the Auger characteristics presented in this paper.

Before installation, the Si targets were etched in $CP4$ etch for 1 minute, then washed in deionized water, re-etched for 20 sec in $CP4$, washed again in deionized water with supersonic agitation, and air dried. The Ge target was etched in a solution of 10 parts HNO_3 and 1 part HF for a total of 11.5 min followed by dipping successively for about 1 minute each in hot xylene, acetone, concentrated HF, and a mixture of 1 part each of HNO_3 and deionized water with 30 sec rinses in deionized water only between each of these steps. Finally, the Ge target was boiled in deionized water for 5 minutes and air dried before being installed in the experimental tube.

In the evacuated apparatus the target surface could be further processed by heating, sputtering, and by the exposure to specific gases. The target was heated by passing alternating current through it. A resistive or reactive load in series with the target served as a current limiter which allowed the heating cycle to start with the applied voltage entirely across the target. When the target temperature rises, the target impedance drops to a very low value and the final current is determined by the series load and the applied voltage. The applied voltage was adjusted with the target shorted to provide the final heating current desired. A current of 8 amp

[2] H. D. Hagstrum, Rev. Sci. Instr. **24**, 1122 (1953).
[3] H. D. Hagstrum, Phys. Rev. **104**, 1516 (1956).
[4] F. G. Allen, T. M. Buck, and J. T. Law, J. Appl. Phys. **31**, 979 (1960).

was required to heat the Si(100) target to 1300°K, 18 amp to heat it to 1570°K.

The arrangement of electrodes for sputtering the semiconductor target is shown in Fig. 1 and in closeup in Fig. 3. A thermionic arc is run between the filament Q and the sphere S at about 60 v and 120 ma in neon at a pressure near 10^{-2} mm Hg. The shield P prevents evaporation products from Q from striking the target. When the target T is put at a potential 100 volts negative with respect to the plasma, sputtering proceeds over the entire surface of the target and its supports at an ion current density of 3 to 5 ma cm^{-2}. Material sputtered from the metal supports or shield P cannot land directly on the front face of the target. There is no evidence that foreign material migrates to this front face. The sputtering method resembles that used extensively by Wehner and his co-workers[5,6] and is the same as that used with a tungsten target in a test of sputtering as a means of cleaning solid surfaces.[7] From the published sputtering yield of about 0.1 germanium atom per neon ion[6] one calculates for the present experiment a sputtering rate of about 1.5 monolayers per second. Thus sputtering for 60 seconds, which was the normal procedure, removed about a hundred monolayers from the surface of the solid. The use to which sputtering was put in this work is discussed in Sec. V.

Resistance of the Si(100) and Ge(111) targets at room temperature was measured periodically during the course of the experiment. The resistance change accompanying cooling of the filament after a flash to high temperature was also measured. These data are also discussed in Sec. V.

Evacuation procedure and the vacuum conditions achieved are similar to those reported in earlier work.[1,2] In the Si(100) experiment, chronologically the first, background pressures were in the 10^{-10} mm Hg range. During one of the bake-out procedures in the Si(111) experiment the apparatus sprang a small leak in a brazed joint between copper and steel parts as a result of crystallization of the brazing material caused by repeated expansion on heating. After repairing the leak with Dow-Corning No. 806 silicone resin the apparatus was baked no hotter than 150°C and the pressure in the apparatus remained near 1×10^{-9} mm Hg. It can be said categorically that this condition was not the result of a minute leak remaining in the vacuum envelope. The total yield and kinetic energy distribution of the Auger electrons ejected by 10 ev He^+ ions, for example, when measured as a function of time after cleaning the surface were always found to change slowly when exposed to the adsorbable gases present as background in the apparatus or admitted as impurities with the noble gases used. During the Ge(111) experiment at one point the kinetic energy distribution for He^+ ions (10 ev) was found to undergo almost no detectable change on exposure of the target for 28 days to the background gases at a pressure reading of 1×10^{-9} mm Hg. When O_2 was admitted to the system at a pressure of about 1×10^{-7} mm Hg, on the other hand, a drastic change was observed in a matter of a few hours (see Sec. V).

Currents to electrodes S and T were measured by means of Cary vibrating reed electrometers. The electrometer used to measure I_S was grounded, that measuring I_T was operated off ground by the voltage V_{ST}.

We shall turn now to a discussion of the experimental methods of measuring total yield, γ_i, and kinetic energy distribution, $N_0(E_k)$, and a report of results for the atomically clean surfaces. We shall return in Sec. V to a documentation of the state of the target surfaces during these experiments.

III. MEASUREMENT OF TOTAL ELECTRON YIELD, γ_i

Both γ_i and $N_0(E_k)$ are obtained from measurements of the quantity $\rho=I_S/(I_T+I_S)$ at different values of the voltage, V_{ST}, between target T and electron collector S. In the expression for ρ, I_S, and I_T are the algebraic values of the currents to the electrodes S and T,

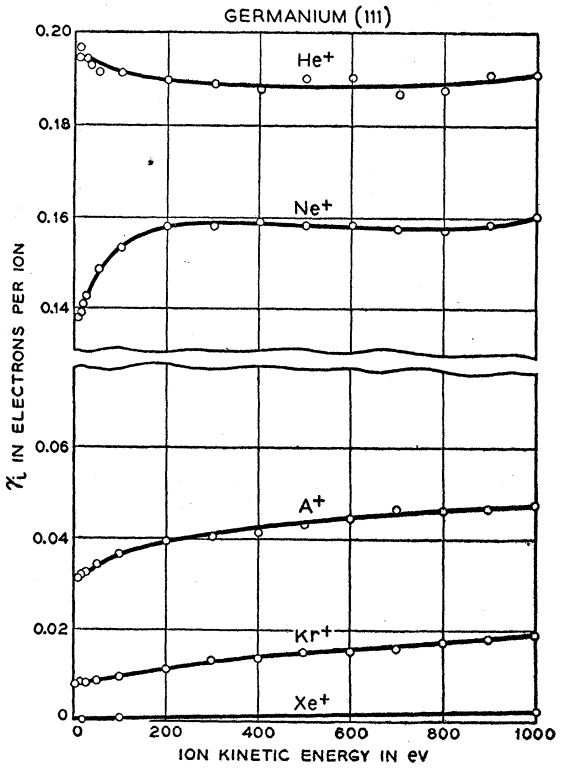

FIG. 4. Plots of total electron yield, γ_i, as a function of incident kinetic energy for the five singly charged ions of the noble gases incident on the atomically clean and annealed (111) face of a germanium crystal.

[5] G. K. Wehner, *Advances in Electronics and Electron Physics* (Academic Press, New York, 1955), Vol. 7, p. 239; Phys. Rev. **108**, 35 (1957).

[6] N. Laegreid, G. Wehner, and B. Meckel, J. Appl. Phys. **30**, 374 (1959).

[7] H. D. Hagstrum and C. D'Amico, J. Appl. Phys. **31**, 715 (1960).

TABLE I. Total electron yields, γ_i, in electrons per ion.[a]

Ion	Ion K.E. (ev)	Ge(111)	Si(111)	Si(100)	W	Mo
He^+	10	0.196	0.188	0.172	0.289	0.300
	100	0.191	0.180	0.168	0.263	0.274
	1000	0.193	0.191	0.178	0.252	0.263
Ne^+	10	0.138	0.128	0.115	0.213	0.254
	100	0.144	0.145	0.131	0.246	0.281
	1000	0.160	0.181	0.169	0.250	0.306
A^+	10	0.032	···	0.024	0.096	0.122
	100	0.037	···	0.027	0.095	0.115
	1000	0.047	···	0.039	0.099	0.118
Kr^+	10	0.008	···	0.007	0.050	0.069
	100	0.010	···	0.009	0.051	0.061
	1000	0.019	···	0.019	0.061	0.073
Xe^+	10	0.0006	···	0.0005	0.013	0.022
	100	0.0003	···	0.0007	0.012	0.019
	1000	0.002	···	0.0018	0.016	0.025

[a] The data for W and Mo are for polycrystalline ribbons and are taken from the papers of reference 1.

respectively. When S is slightly positive with respect to T ($V_{ST}=1$ v, say) I_S is the total ejected electron current and (I_S+I_T) the incoming ion current. Under these conditions γ_i, the total yield measured in electrons per incident ion, is the negative of ρ.

γ_i data for Ge(111) are given in Fig. 4 and for Si(100) and Si(111) in Fig. 5. In each case the surface is in what is considered to be the annealed atomically clean condition. Data were taken after the target had cooled to within 50°K of room temperature following a high-temperature flash. A small percentage of the ejected electrons escape through the entrance aperture to electrode S when V_{ST} is negative. However, this is well within the overall estimated value of 5% for the accuracy and reproducibility of the data and so has not been corrected for.

Some variability from curve to curve was observed for the γ_i of Ne^+ on Si(111) and Si(100) above 600 ev. This more rapidly rising part of the curve was not reproducible and is not understood. Some runs yielded results indicated by the dashed curve for the Si(100) surface. As the Si(111) experiment proceeded a small decrease in γ_i for He^+ and Ne^+ was observed as is discussed in Sec. V. The Si(100) and Ge(111) results were very stable, however.

Some of the electron yield data are given in Table I. Here the results are compared with those published earlier for tungsten and molybdenum.

IV. MEASUREMENT OF ELECTRON ENERGY DISTRIBUTION, $N_0(E_k)$

The kinetic energy distribution, $N_0(E_k)$, of electrons ejected from the target has been determined as $d\rho/dV_{ST}=dI_S/dV_{ST}$ for constant ion current in the range $V_{ST}>0$. The quality of this determination depends on the geometry of target and electron collector and on the extent to which the results are affected by the secondary and tertiary currents associated with the reflection of ions as ions and as metastable atoms at the target. Lukirsky[8] has discussed for a spherical condenser how the retarding potential determination of the energy distribution of electrons released from the inner electrode depends on the relative sizes of inner and outer electrodes. Electrons of initial energy $E_k=eV_0$ released at the inner electrode of radius a will be collected completely at the outer electrode of radius b from a retarding voltage of $V=0$ to $V=(1-a^2/b^2)V_0$. The current to the outer sphere falls to zero in the range $V=(1-a^2/b^2)V_0$ to $V=V_0$. The narrower this retardation range is for monoenergetic electrons the more accurately will the slope of the current versus retarding potential curve reproduce the true energy distribution of electrons ejected with a range of energies. In the present experimental apparatus $b=2$ cm and a may be taken to have a mean value of about 0.5 cm giving $(1-a^2/b^2)=0.94$. Thus an electron of energy $E_k=eV_0$ will be retarded at a voltage V_{ST} which lies

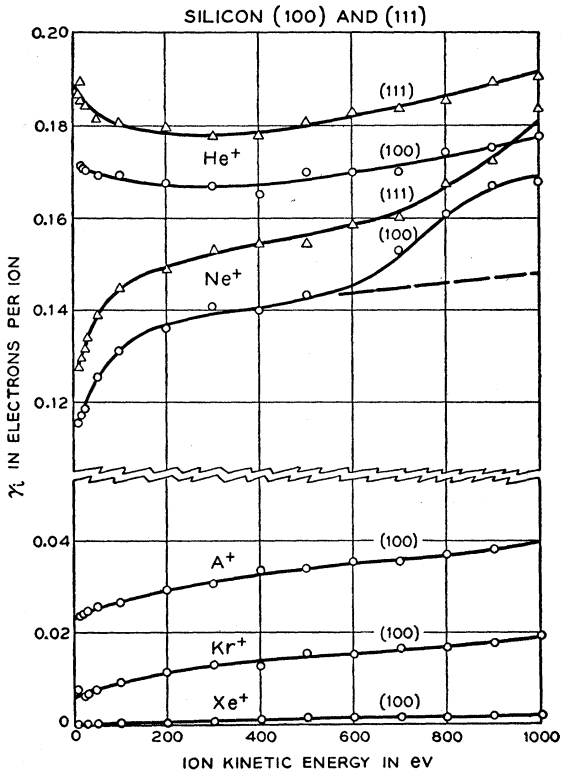

FIG. 5. Plots of total electron yield, γ_i, as a function of incident kinetic energy of the ion for He^+ and Ne^+ on the atomically clean and annealed (111) face of silicon and for all the five singly charged noble gas ions incident on such a (100) face.

[8] P. Lukirsky, Z. Physik **22**, 351 (1924). Note that there is an error in Eq. (8) in this paper. The quantity η is $(b-a)/b$ not $(b-a)/a$ as given. Lukirsky's expression $(2\eta-\eta^2)$ reduces to $(1-a^2/b^2)$.

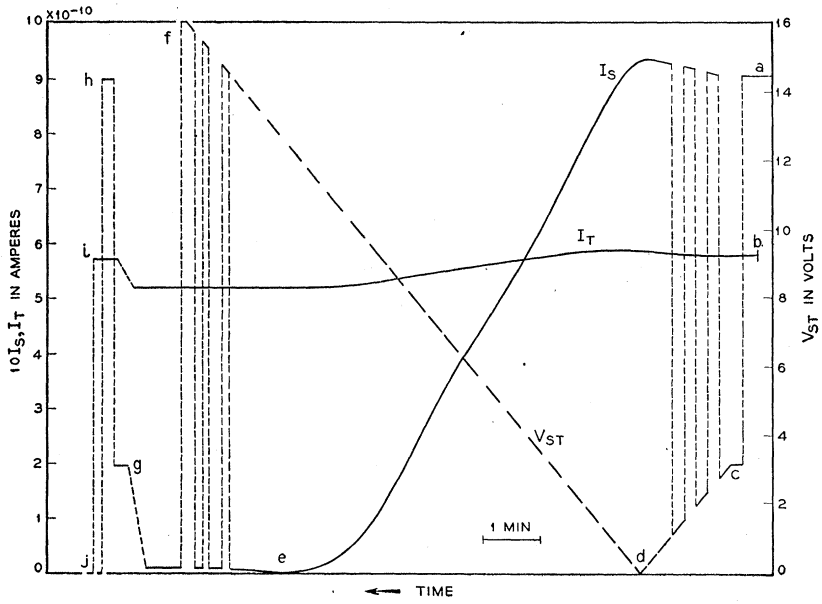

FIG. 6. Tracing of a recorder chart showing the variation of the currents I_S and I_T and the voltage V_{ST} with time. Details are discussed in the text. Since the variation of V_{ST} with time is linear the abscissa scale for the curves of I_S and I_T is proportional to V_{ST}.

within 6% of V_0. Ganichev and Umkin[9] have shown that Lukirsky's results are also valid to within about 1% if the inner sphere is replaced by a disk shaped target of the same radius. This result is quoted for a ratio of outer to inner radii of 10. The effect is undoubtedly greater for smaller ratios of radii but not controlling in the present apparatus. Strong fields at the entrance aperture in the sphere were shown by Ganichev and Umkin to introduce a deviation of as large as 5% from the case of the true spherical condenser. In the present apparatus no such strong fields are employed at the entrance aperture.

The particle currents of ions and metastable atoms reflected from T and of electrons ejected from S by these reflected particles are all small relative to the electron current ejected at T in this experiment except in the case of Xe^+. Furthermore, as discussed elsewhere,[2] those secondary and tertiary particles which are charged are accelerated when $V_{ST}>0$ and their currents are constant and contribute nothing to $d\rho/dV_{ST}$ except when V_{ST} is very near zero. From what has been said about geometry and higher order currents we can be confident that $d\rho/dV_{ST}$ gives an energy distribution $N_0(E_k)$ which approximates the true distribution very well.

In much of the present work I_S, I_T, and V_{ST} were recorded as functions of time while V_{ST} was varied linearly with time from $V_{ST}=-3$ v to $+16$ v. A tracing of such a recording made with a two pen Leeds & Northrup Type G Speedomax recorder is shown in Fig. 6. The recording runs from right to left. Channel 1 records I_S and, intermittently, V_{ST}, and channel 2 records I_T. The recorder chart paper was started with channel 1 recording I_S at a in Fig. 6 and channel 2 recording I_T at b. After about 30 sec channel 1 was switched to V_{ST} which was initially constant at -3 v. At c in Fig. 6 variation of V_{ST} was commenced and over the next minute or so V_{ST} and I_S were recorded alternately. A similar alternate sampling of V_{ST} and I_S with channel 1 was made near the end of the run. This sufficed to sketch in the linear variation of V_{ST}, with time as is shown by the dashed line running from c to d to f in Fig. 6. The V_{ST} signal to the recorder was reversed at d as it went from negative to positive. As V_{ST} became less negative (c to d) both I_S and I_T rose slightly presumably due to lens action at the entrance to the sphere. As V_{ST} became increasingly positive (d to f) I_S was reduced by electron retardation. I_S changed sign from negative to positive at e. When V_{ST} reached $+16$ v its variation was stopped as is seen at f. After about a half minute of further recording of I_S and I_T at $V_{ST}=+16$ v, V_{ST} was returned to $+3$ v and its value recorded by channel 1 at g. Channel 1 was then switched to I_S at h to record again its value at $V_{ST}=+3$ v. Channel 2 recorded I_T at i. It is seen that both I_S and I_T returned very closely to their initial values. The ion current had thus remained constant during the run, a requirement made of all data used in this work. Amplifier zeros were checked at j in Fig. 6.

The kinetic energy distribution $N_0(E_k)$ is to be extracted from the recorded data of Fig. 6 as $d\rho/dV_{ST}$. It is possible to calculate ρ at intervals of V_{ST} by reading off both I_S and I_T. However, the data can be obtained by reading I_S only, if it can be shown that the ion current (I_S+I_T) to the target is independent of V_{ST} as well constant during the time of the run at a given value of V_{ST}. That both of these conditions have been met quite closely is to be seen in Fig. 6. Thus it was possible to calculate the proportionality between I_S and ρ at

[9] D. A. Ganichev and K. G. Umkin, Fizika Tverdoga Tela (U.S.S.R.) **1**, 648 (1959) [translation: Soviet Phys.—Solid State **1**, 590 (1959)].

one point and to use it for the values of I_S read at other points on the curve.

Using a magnifying lens, I_S was carefully read at constant time intervals corresponding to $\Delta V_{ST} \sim 0.4$ v. The data were reduced by an IBM 704 calculator to the quantities V_{ST}, ρ, and $\Delta\rho/\Delta V_{ST}$. An example of the data thus obtained is the $N_0(E_k)=\Delta\rho/\Delta V_{ST}$ plot for 10 ev He^+ ions on Ge(111) in Fig. 7 which was derived as discussed above from the data of Fig. 6. Note that no smoothing of the data has been done here. The recorder chart paper runs at 1 inch per minute so that a complete ρ vs V_{ST} run can be made in about 13 minutes. More rapid change of potentials in the apparatus was found to induce measurable current flow through the sensitive amplifiers. Ion beam and ejected electron currents were of the order of those shown in Fig. 6.

The requirement that ion beam intensity at the target surface be independent of V_{ST} over the range -3 to $+16$ v is a very stringent one, especially for a beam energy at the target surface as low as 10 ev. Constancy of ion energy at the target surface, V_{DT}, requires that the ions enter the sphere with kinetic energy $(V_{DT}+V_{ST})$ which varies with V_{ST}. This variation in voltage must be compensated for at some point in the lens system. Taking up the difference at the beam focus between electrodes K and L_0 (Fig. 1) did not work because it introduced a variable angular spread in the beam between electrodes L_3 and L_4 resulting in a variable beam intensity emerging through the apertures in electrodes $L_{5,6,7}$. After considerable experimentation it was found best to leave all electrode potentials constant through the L-M lens and to accelerate the ions by the requisite amount between electrodes N_1 and N_2 just before they enter the sphere.

The details of how the electrode potentials were set and/or varied is illustrated for the case of ions of 10 ev kinetic energy at the target surface. The L-M lens potentials provided by the circuits previously described[2] were set in this case for $V_{DM}=-6.5$ volts. Thus the ions leave the L-M lens with 6.5-ev kinetic energy. Electrode N_1 is connected to the M potential (midway in potential between M_1 and M_2). Electrodes N_2 and S are grounded, S through the amplifier measuring I_S. T is connected through its amplifier and a voltage source (in the control circuit) putting it permanently 3.5 volts negative with respect to M and making $V_{DT}=-10$ v. A motor driven potential divider is connected between ground (S) and T. Variation of V_{ST} thus varies not only the potential of T with respect to N_2 and S but of M and all other electrode potentials in the lens system with respect to S also. When $V_{ST}=0$ there is an ion acceleration of 3.5 volts between electrodes N_1 and N_2. As V_{ST} is made positive in order to retard the ejected electrons, the ions are accelerated by $(V_{ST}+3.5)$ v between N_1 and N_2 and decelerated by V_{ST} between S and T. It has been shown that the lens action at N_1-N_2 is small enough not to bother us. It is essential, however, that

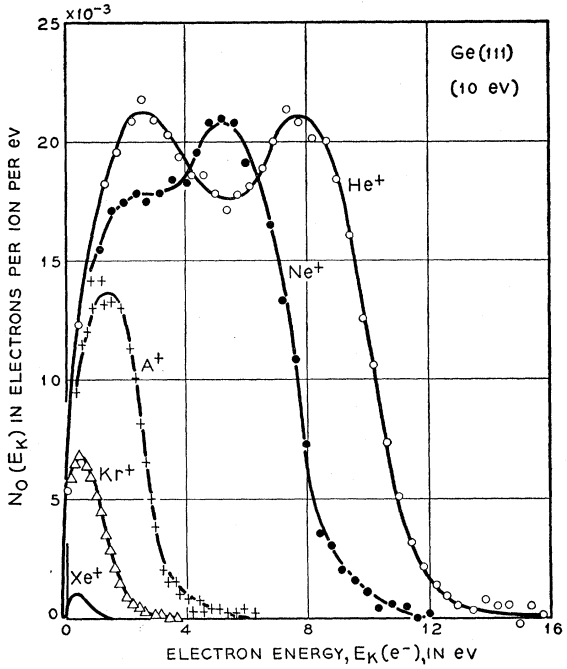

FIG. 7. Kinetic energy distributions, $N_0(E_k)$, of electrons ejected from the atomically clean, annealed, (111) face of germanium by He^+, Ne^+, A^+, Kr^+, and Xe^+ ions of 10 ev incident kinetic energy.

the ions are accelerated between N_1 and N_2 at all times throughout the V_{ST} run. Acceleration of the ion beam between N_1 and N_2 followed by deceleration inside S so close to the final destination of the ions at T results in negligible variation of the total ion current at the target even though V_{ST} is varied from -3 to $+16$ volts. These conditions are critical only at low ion energies where the ion deceleration from S to T is comparable with the ion energy at T.

Data obtained as discussed above for 10 ev singly charged ions of the noble gases incident on the atomically clean and annealed (111) face of germanium are given in Fig. 7. In the case of Xe^+ the effect of reflected ions was an appreciable fraction of the ejected electron current. The $N_0(E_k)$ curve shown for Xe^+ in Fig. 7 is an estimated distribution based on a reasonable disentangling of the two effects in the retarding potential data.

$N_0(E_k)$ distributions for 10 ev He^+ and Ne^+ ions incident on clean and annealed Si(111) are shown in Fig. 8. These data were taken as described above for Ge(111). The data for Si(100) given in Fig. 9, however, were obtained by one of the methods used in earlier experiments. I_S and I_T were read individually at a series of V_{ST} values set manually. When ρ, $\Delta\rho$, and $\Delta\rho/\Delta V_{ST}$ are calculated point by point, greater scatter than that in Figs. 7 and 8 is obtained in the differentiated data. This is to be seen in published data for the refractory metals.[1] In the present work the ρ vs V_{ST} data were plotted to a large scale and a smooth curve drawn through the points. A new set of ρ data were read from this curve and used to obtain the curves of Fig. 9. Here,

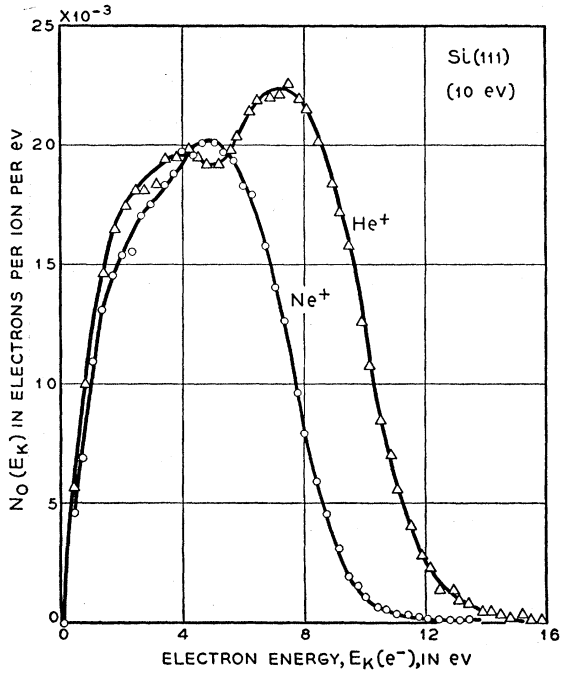

FIG. 8. Kinetic energy distributions of electrons ejected from atomically clean and annealed Si(111) by He^+ and Ne^+ ions of 10 ev incident kinetic energy.

as for Ge(111), the Xe^+ distribution is estimated. That a difference in $N_0(E_k)$ was observed with change of crystal face for silicon is shown in Fig. 10 where the 10 ev He^+ data for Si(111) and Si(100) are compared. A similar change is evident in the data for Ne^+ ions.

Measurements of $N_0(E_k)$ for electrons ejected by ions of initial kinetic energy greater than 10 ev have also been made. A sample of these data for He^+ ions on Ge(111) is given in Fig. 11. The form of the N_0 function is seen to be modified considerably and in an interesting fashion by the increase in ion kinetic energy. Similar data are available for the Si(111) and Si(100) surfaces and for other singly charged noble gas ions.

V. STATE OF THE TARGET SURFACES

A careful attempt has been made in this work to document the state of the target surfaces. As indicated above, the targets were etched before installation and could be further processed by heating, sputtering, and exposure to specific gases after the apparatus was evacuated. Data relating to the state of cleanliness, structure, and temperature of the surfaces at the time the Auger measurements were made were obtained in the following ways:

(1) The Auger characteristics, γ_i and $N_0(E_k)$, were measured for the initial surface and as the initial cleaning of the surface by heating and/or sputtering proceeded.

(2) γ_i and $N_0(E_k)$ were determined as functions of time during which the target, initially clean, was exposed to background gases and to specific gases admitted to the apparatus.

(3) Target resistance at room temperature was monitored during the experiment.

(4) Target resistance and γ_i were measured during the cooling period after a high-temperature flash.

(5) At the conclusion of the Si(100) and Si(111) experiments, these targets were looked at by means of electron diffraction and were photographed under high magnification optically and by means of the electron microscope using carbon replica techniques.

Before any attempts were made to clean them, all three target surfaces showed Auger characteristics dras-

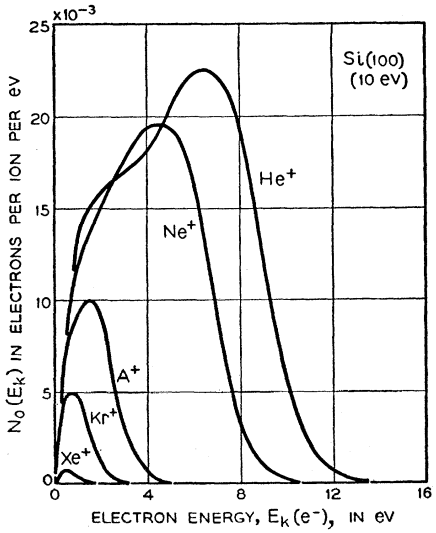

FIG. 9. Kinetic energy distributions of electrons ejected from atomically clean and annealed Si(100) by 10 ev singly charged ions of the noble gases.

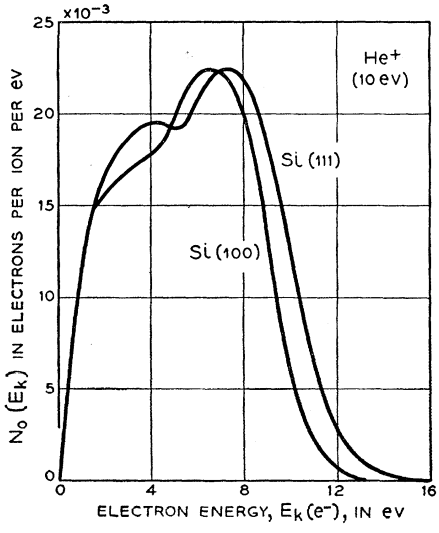

FIG. 10. Comparison of the $N_0(E_k)$ distributions for 10 ev He^+ ions incident on the (100) and (111) faces of silicon. These curves are the same as those in Figs. 8 and 9.

tically different from those shown in Figs. 4–9. Auger data for silicon in the contaminated condition have been published in a paper with Allen, Eisinger, and Law[10] in which cleaning of the surface by heating is discussed. For germanium such data are being published elsewhere.[11] Details may be obtained by reference to the papers cited; only a brief statement of the cleaning procedures used will be given here.

The Si(100) target was cleaned by heating only.[10] Attainment of the atomically clean condition required heating initially to 1530°K. Subsequent thermal restoration of the clean surface could be accomplished at temperatures as low as 1100°K for a 60 second flash. At the time the data reported here were taken the Si(100) target had been heated for a total of several hours at 1570°K. Of course, considerably more heating at lower temperatures had occurred.

The Si(111) target surface was treated in the following way. After some initial heating to outgas the material at temperatures below 1000°K the target was sputtered three times for a total of 180 seconds before the arc filament Q burned out. This treatment produced a marked change in the surface, as indicated by the Auger characteristics, in the direction of the atomically clean surface. There is no reason to believe that the atomically clean condition would not have been completely reached by further sputtering under improved conditions as the tube, in particular the target vicinity, cleaned up. After the arc filament burned out cleaning was done by high temperature heating alone. Considerable further heating at lower temperatures and heating to 1570°K for a total of several minutes had occurred at the time the data given in Figs. 5 and 8 were taken. As is discussed below considerable further heating to 1570°K produced a small change in the measured results.

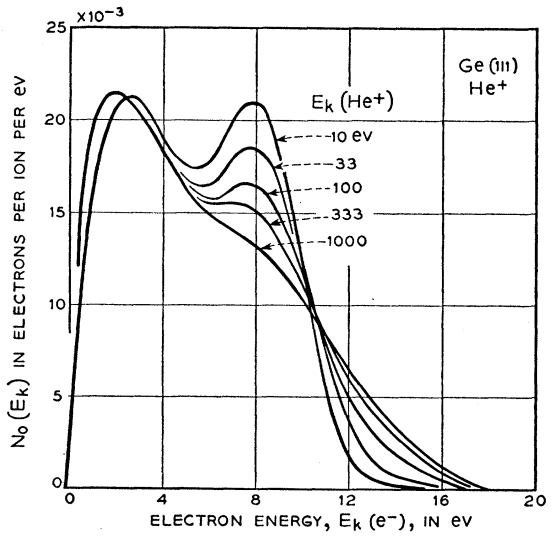

FIG. 11. Variation of the $N_0(E_k)$ distribution for He^+ on Ge(111) with incident ion kinetic energy, $E_k(He^+)$.

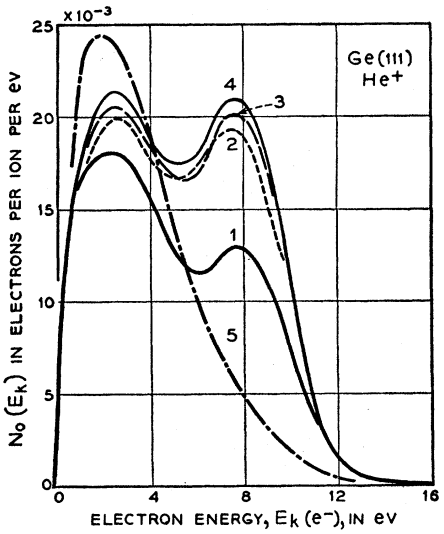

FIG. 12. Several $N_0(E_k)$ distributions for 10 ev He^+ ions incident on the Ge(111) face in various conditions. Curve 1 is the final result of heating to 1170°K (40°K below the melting point) for about three hours. A single sputter of one minute duration (no annealing) took the distribution from curve 1 to curve 2. Curve 3 was taken immediately after the 4th sputter (one minute duration, no anneal). The target was then heated for one minute to 1170°K after which curve 4 was taken. Curve 5 is the distribution after the atomically clean surface has been exposed for 4 hours to oxygen at a pressure of 1×10^{-7} mm Hg.

As has been reported[11] an attempt was made to clean the Ge(111) target by heating only. It was found that heating to within 40°K of the melting point only partially cleaned the surface (Fig. 12); sputtering was required. After this had occurred, cleaning by heating could be accomplished by a 60 second flash to temperatures in the range 600–800°K even after exposure to oxygen. The germanium target had been heated for about 3 hours to 1170°K and sputtered 4 times for a total of 240 seconds at the time the data given here were taken.

Each semiconductor target when atomically clean was reactive to oxygen but much less so to the background gases in the instrument. Some of these results have been reported[10,11]; others will be published later. Little difference was found when the surface was deliberately cooled slowly (over a period of about 2 hours) or cooled as rapidly as radiation and end cooling would allow. In the latter case, as will be seen, the target required several minutes to cool from the high temperature to about 50°K above room temperature. We thus consider the data given here to be representative of the surface in a reasonably well annealed condition. However, we must conclude that the Auger process is not particularly sensitive to surface roughness or damage because data taken immediately after sputtering the

[10] F. G. Allen, J. Eisinger, H. D. Hagstrum, and J. T. Law, J. Appl. Phys. **30**, 1563 (1959).

[11] H. D. Hagstrum, to appear in the *Proceedings of the Second Conference on Semiconductor Surfaces*, held December, 1959, and in J. Phys. Chem. Solids.

Ge(111) target did not differ greatly from what was observed after careful annealing. Results illustrating this point are given in Fig. 12. Here $N_0(E_k)$ distributions for 10 ev He^+ ions are shown after heating only (curve 1), after sputtering only (curves 2 and 3), after sputtering followed by annealing (curve 4), and after exposure for four hours to oxygen at 1×10^{-7} mm Hg (curve 5). This is taken as evidence that heating only will not clean the surface as etched and that reaction with oxygen profoundly alters the electronic states in which electrons reside at the surface.

Once the atomically clean condition had been achieved the results were very stable for the Si(100) and Ge(111) targets. Repeated measurements of $N_0(E_k)$ for 10 ev He^+ on Ge(111) gave results which consistently lay in the range between curves 3 and 4 of Fig. 12. During the period when such measurements were taken the Ge(111) surface was sputtered several times and heated for a total of several hours to 1170°K. In the case of Si(111), however, an irreversible change in the results occurred on prolonged heating near the end of the experiment. The γ_i characteristics for both He^+ and Ne^+ ions were found to drop by about 5% with no essential change in the form of the dependence on ion kinetic energy. The change in form of the kinetic energy distribution for 10 ev He^+ ions during this period is shown in Fig. 13. The curve has dropped in area by about 5% and the minimum near 5-ev electron energy has filled in somewhat. Curve 1 in Fig. 13 was taken after the target had been heated for several minutes to 1570°K, curve 2 after 27 minutes more of heating to this temperature. There is no reason to believe that the surface is not atomically clean throughout this period. There are, however, two other changes which most likely occurred during this period. These two changes are: (1) thermal etching of the surface and (2) development of the chemical p layer under the surface of the semiconductor. From the work of Allen, Buck & Law[4] it would appear that a chemical p layer did form during the heating period in question. At the end of the experiment the Si(111) target was found to have a strong p layer extending into the sample about 6 μ.

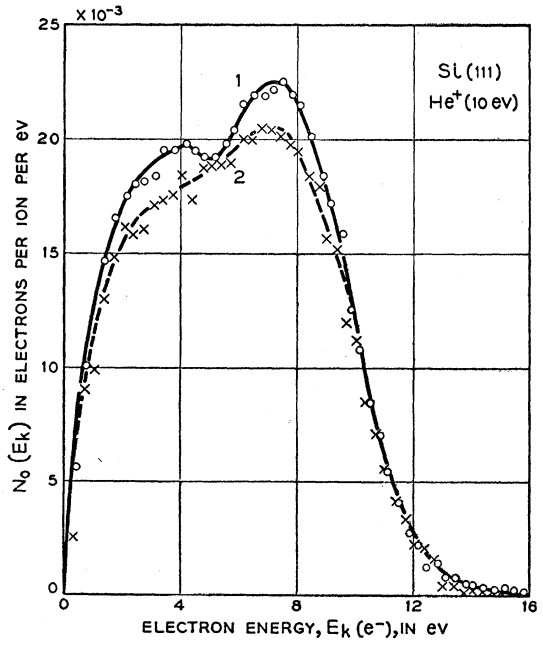

FIG. 13. Curves showing the change in the $N_0(E_k)$ distribution for 10 ev He^+ ions on Si(111) with prolonged heating to high temperature. Curve 1 was taken after considerable heating to temperatures below 1000°K and several minutes to 1570°K. Curve 2 shows the distribution after 27 minutes total additional heating to 1570°K.

Theoretical fitting of kinetic energy distributions shows that the change of $N_0(E_k)$ characteristic from curve 1 to curve 2 in Fig. 13 requires only a very small change in the parameters involved. These two parameters have to do with (1) the ratio of the magnitudes of s type and p type wave functions of valence band electrons outside the surface at the position of the incoming ion and (2) the probability of escape of the excited Auger electrons from the solid. It is certainly not hard to believe that these quantities would be slightly sensitive to changes in surface structure caused by thermal etching. It is more difficult to see any connection with the p layer formation which is undoubtedly very uniform in composition by virtue of surface mobility of the acceptor at the temperatures of heating.[4] One would expect Si to etch thermally because of the high evaporation rate at temperatures to which it can be heated. Ge, on the other hand, evaporates extremely slowly at temperatures just below its melting point. Some facts about thermal etching of the Si(111) surface are presented later in this section.

The second type of information concerning the state of the target surface listed at the beginning of this section has to do with the reactivity of the surface to gas. These matters have been discussed to some extent elsewhere[10,11] and further work is to be published. Suffice it to say here that the Ge and Si surfaces in the atomically clean condition behaved as they should. They are reactive to oxygen (Fig. 12) and show the insensitivity to other common gases observed by other investigators.[12] γ_i was found to change very slowly after the initial cooling period indicating very little interaction with the background gases or with impurities admitted to the system along with the noble gases. It was found that Si exposed to 6×10^{-8} mm Hg of N_2 showed a variation of γ_i with time no more rapid than that measured for background gases alone.

The measurement of target resistance at room temperature during the experiment (Item 3 above) indicated that the resistance changed. The Si(100) target when first measured after some heating to 1550°K had a resistance of about 1800 ohms. This is a higher resistivity by about a factor of three over that specified for the

[12] J. A. Dillon, Jr., and H. E. Farnsworth, J. Appl. Phys. **28**, 174 (1957), **29**, 1195 (1958); J. T. Law and E. E. Francois, J. Phys. Chem. **60**, 353 (1956); J. T. Law, J. Chem. Phys. **28**, 511 (1958); **30**, 1568 (1959).

material from which the target was cut. At the end of the experiment the resistance of this target was about 640 ohms. The most rapid decline came during the period when the target was first heated to 1570°K. The Ge(111) target resistance fell from an initial value near 190 ohms (about the resistivity specified) to a value near 30 ohms. Measurements of target resistance were not made for the Si(111) sample.

The simplest explanation of the drop in target resistance is the formation of the surface p layer due to boron from the pyrex envelope which has diffused into the first 6 μ of the bulk.[4] As indicated above, the presence of the p layer most likely has no detectable effect on the Auger process. The number of impurity atoms resident on the surface to be "seen" by the incoming ion is an extremely small fraction of a monolayer. The p layer found on the Si(111) sample contained about 10^{13} acceptor atoms per cm^2. Even if all of these atoms were concentrated directly on the surface the coverage would be the order of only 0.01. Variation of the electrostatic potential over the first few microns inside the solid should not affect the Auger process which occurs as a result of the overlap, outside the solid, of the wave functions of the ion and of the valence band electrons.

The measurement of target resistance, R_T, and total yield, γ_i, as a function of time on cooling after a flash to high temperature (Item 4 above) yields a number of interesting and informative results. The basic data are plotted in Fig. 14. The principal curves in this figure, labeled Ge(111) and Si(100), show the variation with time of R_T for the targets indicated beginning at the instant the heating current is shutoff. Ge(111) had been heated to 1170°K, Si(100) to 1400°K before cooling. These curves are traces of recordings of the target resistance made with a Model G Leeds and Northrup recorder. A simple constant current circuit was used consisting of a 90 volt battery, the target, and a 165 000 ohm resistor in series. The recorder was connected across the target through a high impedance divider. This circuit was connected to the target at the instant the alternating heating current was shut off and the heating circuit disconnected.

The R_T curves of Fig. 14 have the familiar form and may be used to estimate the target temperature at any given time during the cooling period. This has been done for the Si(100) curve by comparison with Fig. 1 of the paper of Morin and Maita.[13] The R_T curve here was taken when the target had a room temperature resistance of 1620 ohms. This is indicated by the horizontal mark on the right-hand axis. The R_T curve, after passing through the maximum at about 1.6 minutes goes through a shallow minimum at about 6 minutes and, in parts not shown in Fig. 14, rises slowly to the equilibrium value. The conductivity of the target is then about 3.6×10^{-2} ohm^{-1} cm^{-1} which is not far from that of sample 27 of Morin and Maita. The conductivity minimum (R_T maximum) for Morin and Maita's sample occurs at 460°K as seen in their Fig. 1. The Auger data presented in this paper were always taken after several minutes of cooling at which point the target should have been within 50°K of room temperature. Note the slower approach of R_T to normalcy on cooling Ge(111) which reflects its narrower forbidden gap as compared to silicon.

In Fig. 14 three other curves are shown on the same time scale indicating the variation of electron current from the Si(100) target during the cooling period. When the target is very hot one expects thermionic emission to be observable. This current should decay away rapidly during the cooling period. In curve 1 is shown the current to electrode S with V_{ST} accelerating electrons toward S and no ion beam incident on the target. One sees a sharp peak which disappears rapidly. If the ion beam is incident on the target and γ_i is measured as a function of time one obtains curve 2 for 10 ev He$^+$ ions. It shows some evidence of the decaying thermionic current followed by a slower decay of γ_i over a period roughly comparable to that in which the major change in R_T occurs. The amount of thermionic current one can record depends on the rapidity of manual switching from heating circuit to recording circuit.

The main variation in γ_i in curve 2 of Fig. 14 is inter-

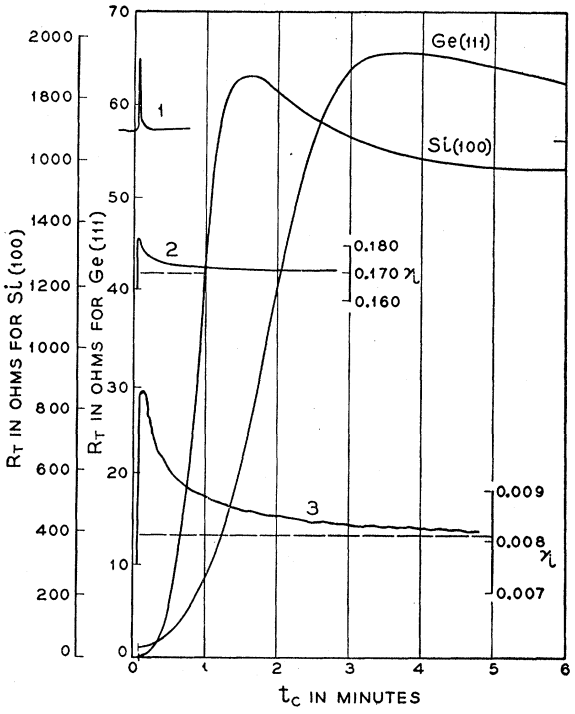

FIG. 14. Tracings of recorder charts showing target resistance, R_T, and electron emission currents as functions of time while cooling from a high-temperature flash. The curves labelled Ge(111) and Si(100) are R_T versus time for the targets indicated. The three inset curves are plotted to the same time scale. Curve 1 indicates the decay of thermionically emitted electon current (no ion beam); Curve 2, the variation of electron current ejected by 10 ev He$^+$ions from Si(100); Curve 3, the variatiou of electron currents ejected by 10 ev Kr$^+$ ions from Ge(111). γ_i scales are indicated for curves 2 and 3 at their right-hand extremities.

[13] F. J. Morin and J. P. Maita, Phys. Rev. **96**, 28 (1954).

preted to result from the decrease in density of thermally excited electrons in the conduction band as the temperature decreases. Conduction electrons, lying higher in energy in the solid and thus closer to the vacuum level than valence electrons will give rise to a higher total yield in the Auger neutralization process than an equivalent number of valence band electrons. This effect is more pronounced for the heavier noble gas ions where γ_i is lower and electron ejection involving the conduction electrons is a greater fraction of the whole. Curve 3 in Fig. 14 shows the variation in γ_i for 10 ev Kr^+ ions incident on Ge(111). Note not only that the effect is greater for the Kr^+ ion but that it persists over a longer time for Ge than for Si by virtue of the narrower forbidden gap in the band structure. In this work, data for the Si targets were taken after at least 2 minutes, for the Ge target after at least 5 minutes of cooling. At this time essentially all conduction electrons have subsided into the valence band and no other effect of the fact that the target is still somewhat above room temperature is expected.

Observations of the Si target surfaces after completion of the experiment (Item 5 above) were as follows. The Si(111) target was looked at by electron diffraction using 40-kev electrons at grazing incidence. These electrons probe an estimated depth of 50 A. Four photographs were taken across the front face of the target. No evidence of reciprocal lattice spots from epitaxial SiC or amorphous SiC were found. A monolayer cannot be detected in this way but comparison with Allen's field emission from Si tips treated as were the targets here indicates that no SiC was present.[10] All photographs showed Kikuchi lines indicating crystalline regularity. There was some general darkening above the reflected spot, however, indicating some amorphous or strained material on the surface at the time the photographs were taken. The target had been exposed to air upon removal from the vacuum system.

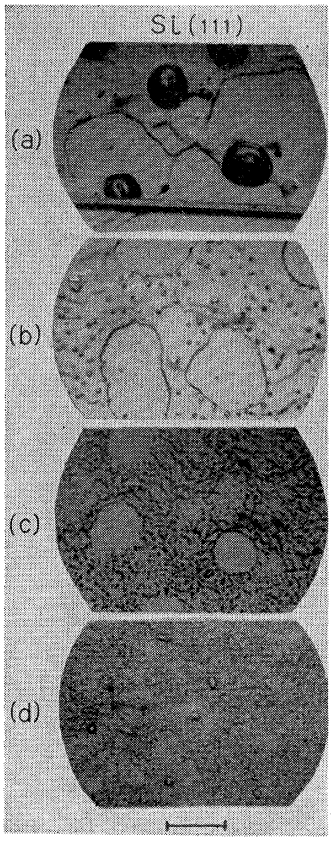

FIG. 15. Four photographs of the Si(111) target surface. Parts (a), (b), (c), (d) on the target face of Fig. 2, respectively. In part (a), a wire of one micron diameter was placed in the field of view to indicate the scale and the direction of the lighting. The line at the bottom of the figure indicates a length of 4 microns on the photographs.

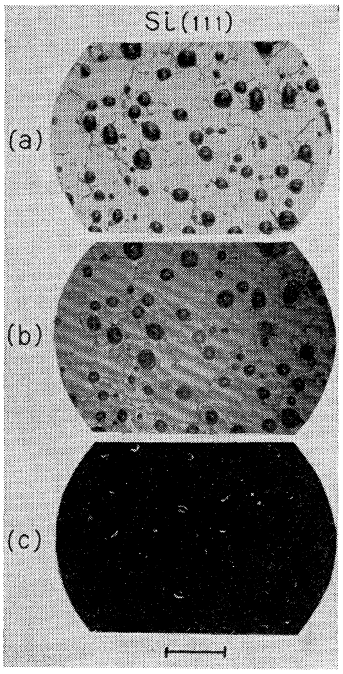

FIG. 16. Photographs of the Si(111) face at point *a* of Fig. 2. Part (a) is with ordinary more or less direct illumination. Part (b) was taken in sodium light with a partially silvered mirror placed on top of the sample. The interference fringes are clearly seen particularly in the flat "lake-like" regions. Part (c) is the same area photographed using dark field illumination. The line at the bottom of the figure indicates a length of 12 microns on the photographs.

The Si(111) surface was also photographed optically. In Fig. 15 are shown four photographs made at the points *a, b, c, d* indicated on the target face in Fig. 2. From the relative positions on the target, it is clear that point *a* had been heated hotter than *b* which had been heated hotter than *c*, etc. It is observed that with more heating the closely pitted structure gives way to larger and larger regions without structure which are interspersed with mounds [see Fig. 15(a)]. It is perhaps true that during the course of the heating the surface at point *a* went through stages not unlike those shown finally by points *d, c, b, a*, in this order.

The central part of the Si(111) target (point *a*, Fig. 2) was photographed in direct illumination [Fig. 16(a)], with a partially silvered flat mirror above it in sodium light to indicate interference fringes [Fig. 16(b)], and with dark field illumination [Fig. 16(c)]. The interferometric technique was identical with that of Batdorf and Smits.[14] Notice how very flat the "lake-like" regions of the surface appear to be. There is little resemblance between Fig. 16(a) and Fig. 11 of Dillon and Farnsworth[15] showing triangular etch patterns developed on the Si(111) face after 200 hours of heating at 1260°K followed by 24 hours at 1350°K.

Three electron micrographs made of carbon replicas of the Si(111) surface shadowed by evaporated ger-

manium are reproduced in Fig. 17. Fig. 17(a) shows a region within one of the flat "lake-like" pits of Figs. 15(a) and 16(a). It is essentially devoid of structure. In Figs. 17(b) and 17(c) are shown "mesa-like" structures which appear with about the surface density of the dark mounds of Figs. 15(a) and 16(a). However, these features are much too small, being about 0.2 micron across, to be identified as the whole of one of the mounds of Fig. 16(a) whose average diameter is about 10 times this amount. Note also that in the dark field illumination of Fig. 16(c) only parts, in many cases only the centers of the dark mounds of 16(a) are evident at all.

It was not possible to find any structure on the electron microscope replicas which could be reliably identified with the whole of one of the dark mounds of Fig. 16(a). One notes that the structures of Figs. 17(b) and 17(c) do, in fact, project from the surface and cast shadows and that the surface rises perceptibly immediately around the base. It is possible that these mounds are like those observed after sputtering by Dillon and Oman[16] and by Meckel and Swalin[17] and attributed to migration of material to and accumulation at an active center on the surface such as the termination of a screw dislocation. One would expect high mobility of surface atoms on heating as well as on sputtering.

There appears to be a reasonably good chance that the surface in the "lake-like" regions of Fig. 16(a) is atomically plane. The interference fringes of Fig. 16(b) are very straight in these regions and the electron micrographs there [Fig. 17(a)] are essentially devoid of structure. Furthermore, in the work of Allen[18] with field emission from Si tips it appears that the (111) region always appears to be flat (emission-free) and tends to grow at the expense of neighboring planes. This correlates nicely with the observation of Batdorf and Smits[14] that the flat "lake-like" regions of Fig. 16(a) grow larger the closer the face normal lies to the (111) direction. Further evidence that the (111) face of a diamond type semiconductor prefers to be flat comes from the work of Bennett and Longini[19] on dendritic crystals of germanium. They find the wide faces of these crystals to be (111) faces which appear to be shiny and mirror smooth. In some instances these faces can be produced in size approaching 1 mm square. One expects that some crystal faces will have lower surface free energy than others.[20] A surface of relatively low surface free energy would become and remain atomically smooth except for steps of atomic dimensions of sufficient density to account for the geometrical angle of the surface with respect to the true crystallographic plane. This is apparently the case for the (111) face of the diamond-type lattice. Faces of higher surface free energy might facet into faces of lower free energy as apparently occurs for the (110) face of tungsten[21] and may well be true for the (100) face of germanium and silicon.

Batdorf and Smits[14] concluded that the steps at the edges of the "lake-like" regions they observed were 200–500 atomic layers high. In Fig. 16(b) in this work one can see flat areas which differ in height by as much as half a fringe corresponding to a minimum difference in elevation of 500 atomic layers.

In Fig. 18 optical photographs in direct and dark field illumination of a point such as *b* of Fig. 2 on the Si(100) target face are reproduced. Note the evidence of pitting. Figure 18 is similar to Fig. 9 of Dillon and Farnsworth[15] obtained after heating for 200 hours to 1260°K but differs markedly from the etch pattern obtained by these investigators after the heating to 1260°K for 200 hours only (their Fig. 8). Most likely a sizeable fraction of the Si(100) surface is made up of areas having surface normals quite far from the (100) direction. However, as we have seen, there is a definite difference

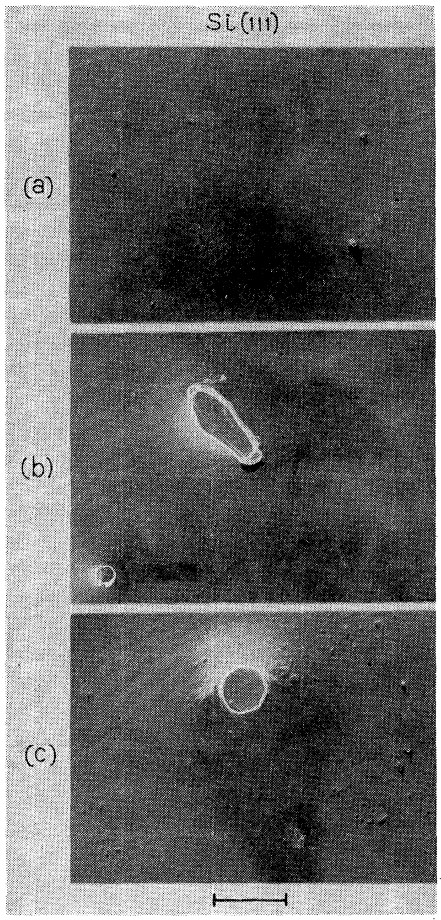

FIG. 17. Three electron micrographs of a shadowed carbon replica of the Si(111) face at points in the vicinity of point *a* of Fig. 2. The line at the bottom of the figure indicates a length of 0.2 micron on the micrographs.

[14] R. L. Batdorf and F. M. Smits, J. Appl. Phys. **30**, 259 (1959). See also W. L. Bond and F. M. Smits, Bell System Tech. J. **35**, 1209 (1956) for further discussion of interferometric techniques.
[15] J. A. Dillon, Jr., and H. E. Farnsworth, J. Appl. Phys. **29**, 1195 (1958).
[16] J. A. Dillon, Jr., and R. M. Oman, J. Appl. Phys. **31**, 26 (1960).
[17] B. B. Meckel and R. A. Swalin, J. Appl. Phys. **30**, 89 (1959).
[18] F. G. Allen (private communication).
[19] A. I. Bennett and R. L. Longini, Phys. Rev. **116**, 53 (1959).
[20] C. Herring and M. H. Nichols, Revs. Modern Phys. **21**, 185 (1949).
[21] M. H. Nichols, Phys. Rev. **57**, 297 (1940).

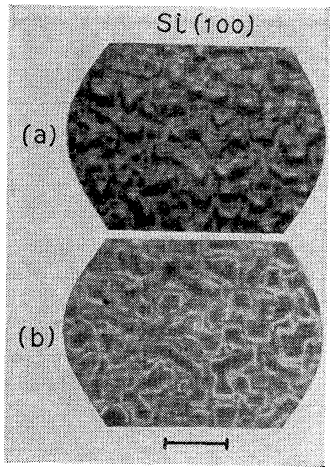

FIG. 18. Photographs of the Si(100) face in direct (a) and dark field illumination (b) at a point on the surface such as *b* of Fig. 2. The line at the bottom of the figure indicates a length of 4 microns on the photographs.

between the Auger characteristics measured for this face and for the Si(111) face. These differences also have the direction and magnitude which theory would predict. Thus the Si(100) target face cannot be made up entirely or even largely of facets of (111) planes. It is clear that one can specify the surface structure of the Si(100) target with much less confidence than that of the Si(111) target.

VI. CONCLUSION

The experimental results given in this paper will form the material for theoretical interpretation in other publications as stated in the Introduction. Only a brief identification of these results with theoretical ideas is attempted here.

The γ_i characteristics of Figs. 4 and 5 resemble in general form those already measured for metals. This is interesting in view of the fact that the electrons involved in the Auger neutralization process are valence band electrons in a semiconductor and conduction band electrons in a metal. It is apparent that the electrons in the highest lying filled band in the solid become involved in these Auger-type processes. The general constancy of electron yield over two orders of magnitude of ion kinetic energy again points to the fact that the energy expended in releasing the electrons from the solid comes basically from the potential rather than the kinetic energy of the ion. The fine structure in the γ_i characteristics is related to the identical features of the theory already published for metals.[22]

The general level of magnitude of the total electron yield from silicon and germanium is a little over half that for the refractory metals. This is the result of the lower electron state density in the valence band of these semiconductors compared to the conduction band of the metals.

The $N_0(E_k)$ kinetic energy distributions of electrons plotted in Figs. 7, 8, and 9 show interesting structure. This can be related to the form of the state density function in the valence band at the surface of the semiconductor. The state density function derives its form in turn largely from the concentration of the two degenerate p electrons in a relatively narrow band at the top of the over-all valence band.[23] The differences between the results for the three surfaces, Si(111), Si(100), and Ge(111) are in the direction and of the magnitude predicted by the theory.

The variation of the $N_0(E_k)$ function with ion kinetic energy shown in Fig. 11 also follows the same general pattern as for the metals. The broadening of the function as ion kinetic energy increases is the result of two factors: (1) the variation of the ground state level of the ion as it appraoches the metal and (2) the Heisenberg uncertainty principle. Both of these effects arise from the fact that the primary result of firing the ion at the surface with greater velocity is to cause the Auger process to occur closer to the solid surface. Theory also predicts in a satisfactory manner this dependence of $N_0(E_k)$ on incident kinetic energy of the ion.

Studies made of the target surface conditions described in this paper indicate that the data presented relate to atomically clean surfaces in an annealed condition. For the (111) faces studied there is good reason to believe that to an incoming ion the surfaces appear to be essentially atomically plane over a large fraction of their area.

ACKNOWLEDGMENTS

It is a pleasure to acknowledge the technical assistance of C. D'Amico during the experimentation. The author is also grateful to Mrs. M. H. Read for performing the 50-kev electron diffraction study, to Miss S. E. Koonce for the electron micrographs, to R. L. Batdorf and K. A. Mills for use of apparatus and assistance while taking the photograph of Fig. 16(b), and to F. G. Allen for measurements of the chemical p layer found on the Si(111) sample.

Note added in proof.—Since submitting this paper further experimentation with the Ge(111) target has been completed and the target removed from the apparatus, inspected, and photographed. In its final state the target shows evidence of surface melting at the center of its front face (the hottest point on heating) and along one of its longer edges. This melting occurred, in all probability, during a heating period of many hours at temperatures thought to be near but not above the melting point. This occurred after all data published in this paper had been recorded. A series of photographs like those of Fig. 15 show the same tendency to form the flat "lake-like" regions with increased heating. However, for germanium only in places very near the surface melted portions does one find as well developed a structure as shown for silicon in Fig. 15(a). Even here the surface tends to look more like Fig. 15(b) than 15(a). Over most of the surface which the ion beam strikes, the Ge(111) surface looks most like Fig. 15(c). These observations would appear to be consistent with the fact that germanium cannot be heated as hot nor evaporated as rapidly as can silicon. The occasion of a future publication will be used to give further details on these observations.

[22] H. D. Hagstrum, Phys. Rev. **96**, 336 (1954).

[23] H. D. Hagstrum, J. Phys. Chem. Solids **8**, 211 (1959).

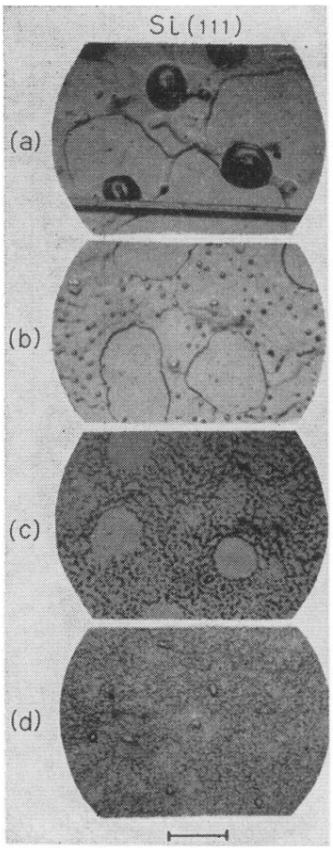

FIG. 15. Four photographs of the Si(111) target surface. Parts (a), (b), (c), (d) on the target face of Fig. 2, respectively. In part (a), a wire of one micron diameter was placed in the field of view to indicate the scale and the direction of the lighting. The line at the bottom of the figure indicates a length of 4 microns on the photographs.

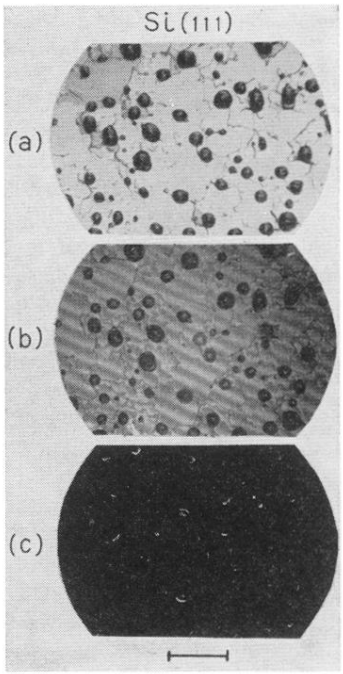

FIG. 16. Photographs of the Si(111) face at point *a* of Fig. 2. Part (a) is with ordinary more or less direct illumination. Part (b) was taken in sodium light with a partially silvered mirror placed on top of the sample. The interference fringes are clearly seen particularly in the flat "lake-like" regions. Part (c) is the same area photographed using dark field illumination. The line at the bottom of the figure indicates a length of 12 microns on the photographs.

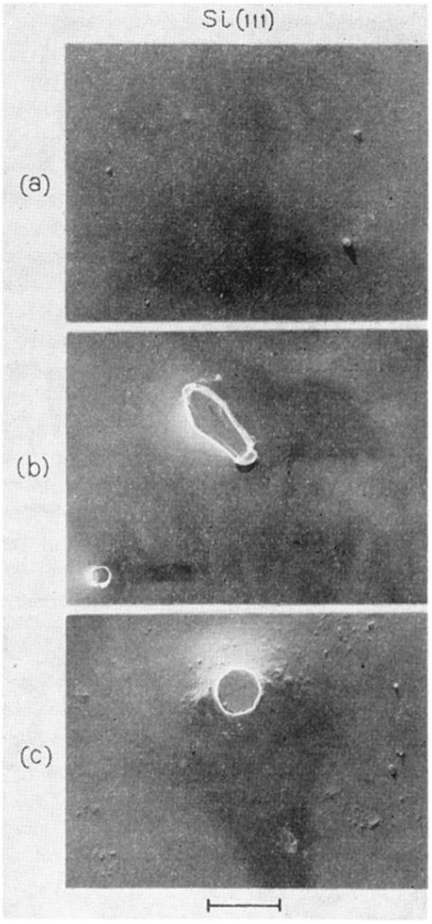

FIG. 17. Three electron micrographs of a shadowed carbon replica of the Si(111) face at points in the vicinity of point *a* of Fig. 2. The line at the bottom of the figure indicates a length of 0.2 micron on the micrographs.

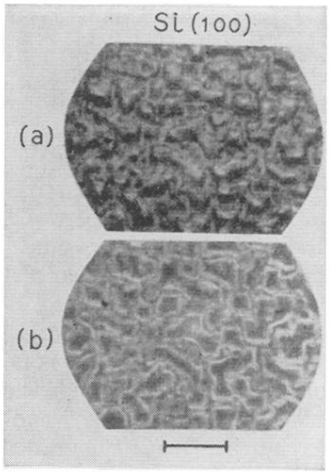

FIG. 18. Photographs of the Si(100) face in direct (a) and dark field illumination (b) at a point on the surface such as *b* of Fig. 2. The line at the bottom of the figure indicates a length of 4 microns on the photographs.